Oxidation of Metals, Vol. 66, Nos. 1/2, August 2006 (© 2006)
DOI: 10.1007/s11085-006-9028-8

First Stages of Internal Oxidation in Ag-0.29 and 2.89 at. % Mg Single-Crystal Alloys

L. Charrin*[$], P. Gergaud*, G. Gonzalez[†], A. Mazuelas[‡] and A. Charaï*

Received September 21, 2005; revised February 3, 2006

Internal oxidation of Ag-0.29 and 2.89 at.% Mg alloys was studied by in-situ X-ray measurements at 300°C. The kinetics and lattice-parameter changes as a function of time are discussed in terms of the formation of elementary MgO species and non-stoichiometric clusters, during the first stages of oxidation. Studies were made using synchrotron radiation on single-crystal samples. The distorted zone, formed near the surface, was detected by measuring the position and the intensity of the (022) silver peak in the solid-solution alloy. From the diffraction-peak changes, information is deduced on the growth kinetics of the expanded layer. Oxygen diffusivity in silver, C_0D_0, is calculated on the basis of Wagner's law. At an early stage, the oxygen diffusivity is slightly lower than the theoretical value. During a second stage, accelerated kinetics give a very high C_0D_0 value. We determined the O/Mg ratios at different stages during oxidation.*

KEY WORDS: Silver-magnesium alloys; internal oxidation; X-ray diffraction; oxygen diffusivity

*TECSEN, UMR CNRS 6122Univ. Paul Cézanne – Aix Marseille III, 13397, Marseille Cedex 20, France.
[†]Instituto de Investigaciones en Materiales-UNAM A.P. 70-360, 04510, Mexico, Mexico D.F.
[‡]Anomalous Scattering, ID01 Beamline, European Synchrotron Radiation Facility (ESRF), 22038043, Grenoble, France.
[$]To whom correspondence should be sent. e-mail: lcharrin@univ-cezanne.fr

INTRODUCTION

Much work has been performed on the internal oxidation of silver-base alloys [1,2]. From these studies, it appears that the process depends strongly on temperature. At high-temperature,[2,3] the only observed phase is the stoichiometric oxide. Wagner's theory explains this fact by considering that the oxidation kinetics are controlled exclusively by oxygen diffusion.[4] The thickness, ξ, of the internal-oxidation zone increases as a parabolic function of time:

$$\zeta^2 = 2C_o D_o t/\eta C_s \quad (1)$$

where C_oD_o is the diffusivity of oxygen in silver, $\mathbf{C_s}$ the solute concentration in silver and η the ratio between oxygen and solute atoms for a stoichiometric oxide.

Furthermore, at high-temperature and for high-concentration alloys ($\approx$ 2 at.% or more), it has been shown that in silver alloys containing reactive solutes (Sn, Zn, Mg, Cu) there is an important lattice expansion during internal oxidation.[5–8]

At low-temperature (< 420°C), we presented analogous results in dilute Ag–Mg alloys [9,10]. The change with time of the (022) silver diffraction peak was determined and the development of an extra peak (characteristic of an expanded phase) was followed, whose intensity increases as the matrix-peak intensity decreases. A comparison between these results and data obtained by gravimetric measurements [11] shows that sub-stoichiometric clusters (with magnesium excess) are formed, in a first step, without expansion. Matrix distortion occurs, in a second step, according to the evolution of the earliest clusters by the fixation of an oxygen excess (hyper-stoichiometric clusters) during a coalescence process. At variance with the measurements at high-temperature, the stoichiometric phase was never observed at low temperature, at least within the applicable reaction time.

In fact, all these previous studies show that whatever the temperature and composition, no induction period is detected. Oxygen and magnesium atoms react instantaneously, and Mg–O links occur to form very-mobile elementary species MgO^*. Such species could be precursors of sub-stoichiometric clusters $Mg_nO_m (n > m)$ by self-reaction and/or reaction with magnesium-free atoms. Within this model, the oxygen would be the only mobile specie that could be attracted by the surface of these earliest sub-stoichiometric clusters which would become hyper-stoichiometric and produce a lattice distortion of the matrix. At the end of such a process, clusters organize themselves towards the stoichiometric oxide, giving rise to an oxygen release and a relaxation of the silver lattice.[9]

The observation of the first steps of internal oxidation (with hypo- and hyper-stoichiometric cluster formation) is related to the experimental conditions, especially the temperature which must be low enough. Elsewhere, it has been also reported that the solute content and the temperature determine the formation, morphology and size of clusters.[12–15] For instance, at high temperatures, the internal oxidation of dilute alloys ($\approx$ 2 at.% or less) leads to a dispersed oxide within the matrix. The oxidation of more-concentrated Mg alloys leads to the formation of periodic bands parallel to the surface.[12,16,17] Finally among other important parameters, the material microstructure, i.e. the grain size, may strongly influence the kinetics of cluster formation.

The aim of this study was to observe the Ag peak splitting during in-situ oxidation and to follow its evolution versus time. It was intended to collect information about the oxidation kinetics from the earliest stages; this investigation allows also the determination of O/Mg ratios during internal oxidation at low-temperature.

In order to avoid the microstructural effects, we chose to study the internal oxidation in single crystals. The influence of the magnesium content was studied in two different alloys (0.29 and 2.89 at.% Mg).

EXPERIMENTAL PROCEDURE

Polycrystalline Ag–Mg alloys were first prepared by melting Ag (99.999 at.%) and Mg (99.95 at.%) in a graphite crucible, under argon atmosphere, by high-frequency induction. Then, single crystals were made by the Bridgman method, as reported in previous work.[13]

The X-ray diffraction experiments were performed at European Synchrotron Radiation Facility (ESRF) on ID01 beam line with a wavelength of 0.1649 nm. A four-circle goniometer, equipped with a position-sensitive detector spanning a 2.5° angular aperture and having an angular resolution of 0.005° was used. Sample alignments were performed at room temperature. The large goniometer radius (about 1 m) helps in reducing the peak position shift due to sample displacement during heating or cooling. The diffractometer was equipped with a furnace allowing measurements of symmetric and asymmetric reflections because of the dome shape of the beryllium window. To increase the sensitivity of the Bragg-shift measurement, we followed the symmetrical (022) reflection of the Ag(Mg) alloy at a Bragg angle close to 69.6°. Under these experimental conditions, the mean X-ray penetration depth is about 1 μm, and less than 10% of the diffracted beam is provided by a sublayer at 2.5 μm underneath the sample surface. The peak position was followed *in-situ* under isothermal conditions. The

temperature was controlled by a thermocouple fixed to the heater. The samples were heated at 300°C for at least 10 hr.

The X-ray diffraction method employs the lattice-plane spacing d_{hkl} of an $\{hkl\}$ set of planes as an internal-strain gauge.[18] This strain is linked via Bragg's law to the diffraction angles measured on the analyzed sample:

$$\varepsilon = \frac{d - d_0}{d_0} = -\frac{1}{2}\cot\ \mathrm{an}\theta.\Delta 2\theta \tag{2}$$

where ε is the strain along the measured direction, d_0 and θ_0 are, respectively, the lattice spacing and the Bragg angle corresponding to a stress-free state, d and θ are, respectively, the lattice spacing and the Bragg angle corresponding to the stressed sample, and $\Delta\ 2\theta = 2\theta - 2\theta_0$ is the Bragg-angle shift. When oxidation occurs in the Ag(Mg) sample, the measured strain can include both an elastic part due to elastic stress but, also, a chemical strain because of a modification of the stress-free lattice spacing during oxidation of the Mg solute. At such a temperature, Goretta et al. [19] measured a yield stress of Ag-1.2 at.% Mg of 383 MPa after oxidation at 900°C for 4 hr. Assuming a biaxial state of stress σ in the sample, a Young's modulus E of 83 GPa and a Poisson ratio v of 0.37; the out of plane strain $\varepsilon_\perp$ can be estimated from the following relation:

$$\varepsilon_\perp = \frac{-2v}{E}\sigma \tag{3}$$

For an oxidized sample, the out-of-plane strain can be higher than 0.35%. This value is much higher than the value expected from the solid-solution effect (0.06% for 2.89 at.% Mg and 0.006% for 0.29 at.% Mg).

EXPERIMENTAL OBSERVATIONS

Peak-Intensity Variations

During the experiments described above, we followed the peaks corresponding to undistorted and distorted zones inside the sample. From our model [8,9], the undistorted-matrix peak remains unchanged as elementary MgO^* species and hypo-stoichiometric clusters form; the extra distorted diffraction peak is due to the formation of hyper-stoichiometric clusters. Figures 1 and 2 show the evolution versus time of the (022) diffraction peak obtained during internal oxidation at 300°C, respectively, on dilute (0.29 at.%) and concentrated (2.89 at.%) silver–magnesium alloys. We can observe how the Ag–Mg solid-solution peak disappears as the oxidizing

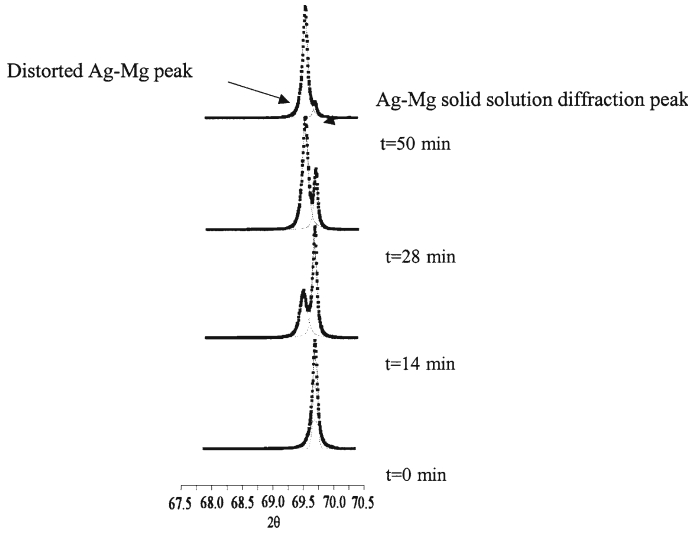

Fig. 1. Ag-0.29 at %Mg alloy. Ag (022) diffraction-peak position as a function of time, during oxidation.

front progresses; in both samples, one can see that the extra broadened peak is located at a smaller Bragg angle, corresponding to the development of a distorted zone near the surface. Whatever the alloy, the diffraction peaks are sufficiently separated to give evidence of the undistorted and distorted zones. In the Ag-0.29 at.% Mg alloy, after 60 min, only the peak corresponding to the expanded layer remains. The same process takes place about 180 min for the Ag-2.89 at.% Mg alloy. The extra diffraction peak appears as the dilute alloy is exposed 6 min under air atmosphere. This phenomenon requires more than 15 min to be observed for the more-concentrated alloy. This comparison may be explained by the difference in both oxygen flux and velocity of the oxidation front. This velocity V is inversely proportional to the solute concentration.[1,11] During internal oxidation of silver–magnesium alloys, velocity is expressed by the first derivative with time of Eq.1, i.e.: $V = C_o D_o / C_{Mg} \eta \zeta$[11], where C_{Mg} is the magnesium concentration in silver.

Kinetics Investigation: C_0D_0 Calculations

The thickness of the expanded layer, h_{ox}, is deduced from the relative intensity of the peaks as follows:

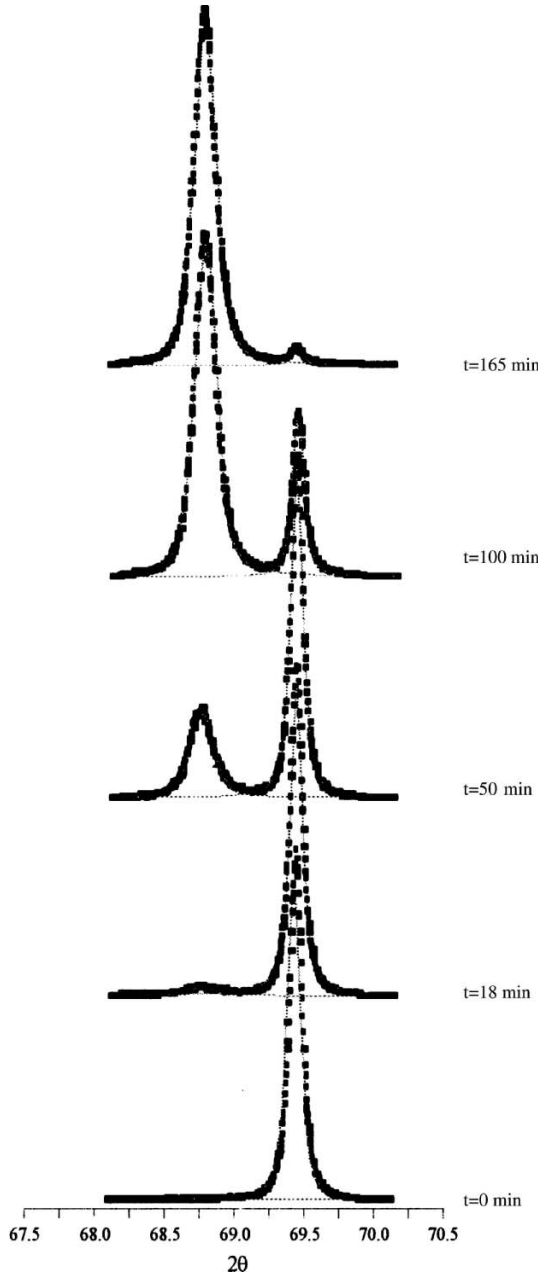

Fig. 2. Ag-2.89 at %Mg alloy. Ag (022) diffraction-peak position as a function of time, during oxidation.

$$h_{ox} = \frac{\sin(\theta)}{\mu} \ln \frac{I_{unox} + I_{ox}}{I_{unox}} \tag{4}$$

where μ is the linear-absorption coefficient of silver and is equal to 2.3 10^5 m^{-1}. I_{ox} and I_{unox} are the peak intensities of the oxidized layer and of the non-oxidized layer, respectively.

The thickness of the expanded layer is also related to the oxygen diffusivity through the Wagner equation (Eq. l):

$$h_{ox} = 2C_o D_o t / C_{Mg} \eta \tag{5}$$

From Eq. 4 and 5, the diffusivity in the oxidized layer C_0D_0 can be determined:

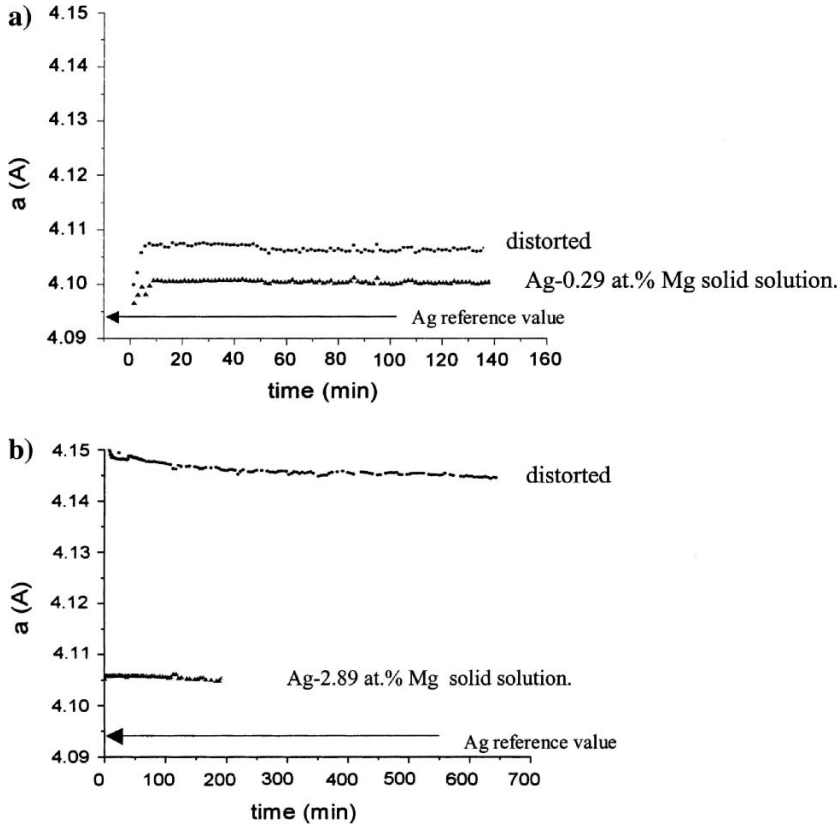

Fig. 3. C_0D_0 values as a function of $t^{0.5}$. (a) Ag-0.29 at% Mg. (b) Ag-2.89 at% Mg.

$$\left(\frac{2C_{\mathrm{o}}D_{\mathrm{o}}}{\eta C_{\mathrm{Mg}}}\right)^{0.5} t^{0.5} = \frac{\sin(\theta)}{2\mu} \ln\left(\frac{I_{\mathrm{ox}} + I_{\mathrm{unox}}}{I_{unox}}\right) \quad (6)$$

Plotting the right hand of Eq.6 as a function of $t^{0.5}$, the C_0D_0 value can be deduced from the slope of the straight line (Fig. 3). For the dilute alloy (0.29 at.% Mg) we find 1.59×10^{-15} cm^2/s. For the more-concentrated alloy (2.89 at.% Mg), the curve is not linear with temperature, and two distinct slopes can be extracted for the C_0D_0 values. These values are 7.24×10^{-15} cm^2/s and 1.83×10^{-12} cm^2/s, respectively.

By comparison of these results with the value (4.73×10^{-13} cm^2/s) tabulated by Eichenauer and Müller[14] for silver, we observe slower kinetics, in each sample, for short oxidation times (less than 60 min). In the case of longer oxidation times, if the phenomenon is still observable (concentrated alloys), the C_0D_0 value is larger than reported by Eichenauer and Müller's measurements.

Peak-Position Variations

The initial lattice parameters of the unoxidized matrix obtained on the samples at 300°C and at the first annealing stage are 0.41005 nm and 0.41060 nm for the dilute and more-concentrated alloys, respectively. From the peak positions (Fig. 4), the lattice-parameter changes of the undistorted matrix and of the expanded layer were plotted as a function of time. These reported values indicate that the lattice-parameter of the unoxidized solid solution remains unchanged during the experiment. The results also indicate that the lattice-parameter expansion of the oxidized matrix is proportional to the solute concentration which can explain the different values $\Delta\mathbf{a}/\mathbf{a}_{\mathbf{Ag(Mg)}}$ observed between 2.89 at.% Mg ($\Delta\mathbf{a}/\mathbf{a}_{\mathbf{Ag(mg)}} > 10^{-2}$) and 0.29 at.% Mg ($\Delta\mathbf{a}/\mathbf{a}_{\mathbf{Ag(Mg)}} = 1.7 \times 10^{-3}$) alloys. After the first minutes of oxidation a maximal value of the lattice parameter is observed; the increase (Fig. 4(a)) of the lattice parameter ($\mathbf{a}_{\mathbf{max}} = 0.41075$ nm) is followed, in the dilute alloy, by the displacement of the extra-peak. Such observation is impossible in the more-concentrated alloy (Fig. 4(b)), in which the fast and large increase ($\mathbf{a}_{\mathbf{max}} = 0.41500$ nm) is not recordable.

The distorted matrix reaches a maximal lattice parameter depending on solute concentration. This value can evolve for longer oxidation times. In the dilute alloy, the decrease after a moderate expansion of the lattice parameter (Fig. 4(a)) is weak ($\mathbf{a}_{\mathbf{max}} - \mathbf{a}_{\mathbf{final}} = 0.41075 - 0.41055$ nm); in the more-concentrated alloy the highest maximum value is followed by a more important decrease ($\mathbf{a}_{\mathbf{max}} - \mathbf{a}_{\mathbf{final}} = 0.41500 - 0.41450$ nm) (Fig. 4(b)). These

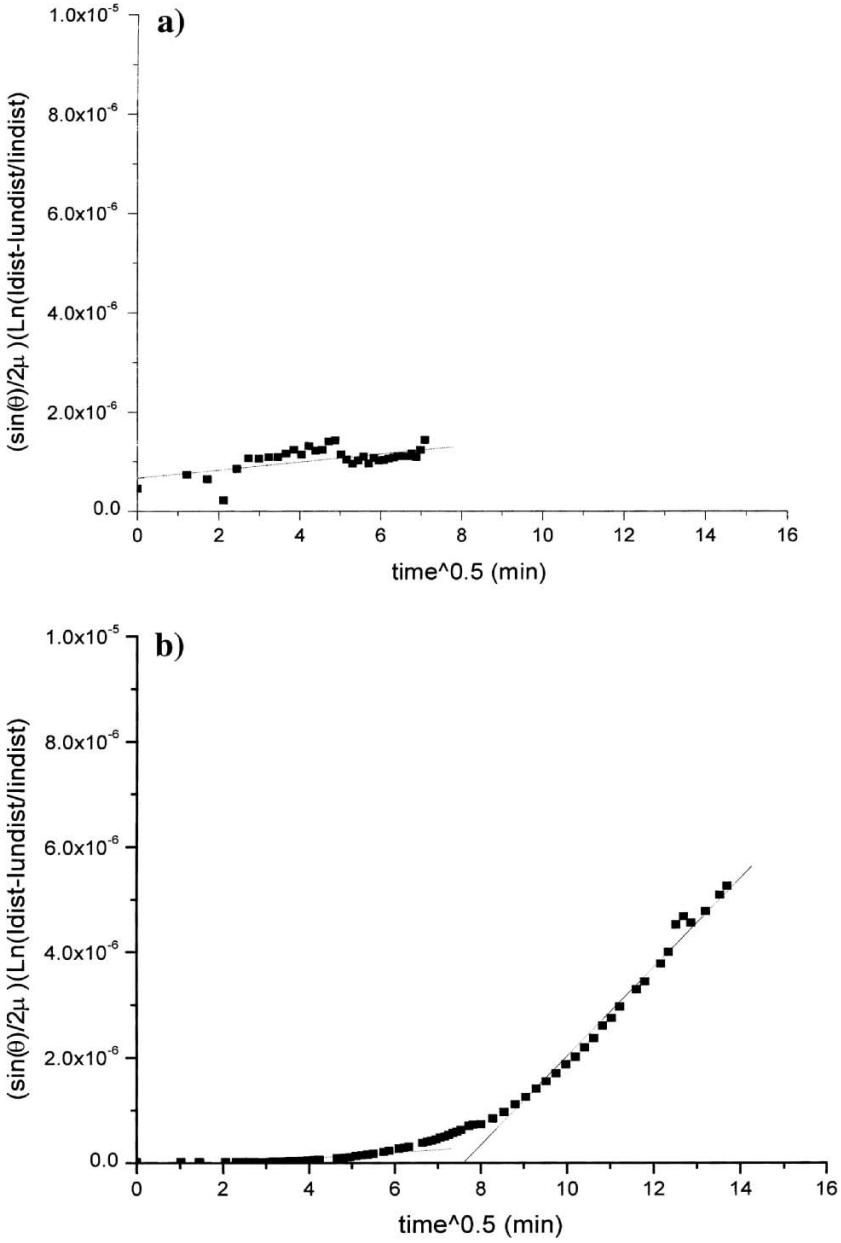

Fig. 4. Lattice-parameters variation as a function of time during in situ oxidation.(a) Ag-0.29 at% Mg. (b) Ag-2.89 at% Mg.

observations seem to be in agreement with the results of a previous study realized by ex-situ measurements, on a polycristalline Ag-1 at.% Mg alloy.[6]

DISCUSSION

Kinetics: Oxidation Front and Expanded Layer

The C_0D_0 values calculated in this investigation give evidence that the oxygen diffusivity depends on the oxidation time. During short oxidation times (about 60 min), we measured at the surface of the samples the evolution of two diffracted peaks owing to the oxidized matrix and to the non-oxidized matrix. In the dilute alloy, this last one disappears; further calculations of C_0D_0 values is then impossible. In the Ag-2.89 Mg, the two peaks are observable during a longer time (about 180 min). This is in agreement with Wagner's theory, stating that the thickness of the oxidized zone varies inversely with the square root of the solute concentration.

In the first stages of oxidation, the matrix remains undistorted as hypo-stoichiometric clusters are formed by rapid fixation of oxygen. The extra-distorted diffraction peak is due to the formation of hyper-stoichiometric clusters (i.e. oxygen excess), in the next stage, in which an evolution of the initial clusters takes place by a coalescence process. On the basis of such assumptions, the observed expansion is related to the oxygen excess. This expansion is due to a progressive fixation of an oxygen excess followed by a partial release allowing reorganization of the clusters.[9–11] From Wagner's law, the expected growth rate ($V = C_oD_o/C_{Mg}\eta\zeta$) of the expanded layer is infinite at zero time of oxidation which is not in agreement with our experimental results.

Ex-situ X-ray measurements realized in a previous study,[9] (on Ag-0.5 and 1 at.%), lead to the conclusion that the thickness of the expanded layer varies as $\mathbf{t^n}$ with $\mathbf{n} > 1$; so the experimental growth rate is initially very low (about 0, for $\mathbf{t} = 0$); in this last case, it is expected that experimental and theoretical growth rate curves cross each other for a higher value of **t**.

First Step

The results obtained for the 2.89 at.% Mg alloy are in good agreement with the oxidation process previously proposed.[9,17] During the first 15 min, corresponding to the formation of the hypo-stoichiometric species in a non-expanded layer, the extra diffraction peak is not observed. During these 15 min, the theoretical depth of the oxidation front, determined by Eq. 1 (using a η value equal to 1), is at about 1.2 μm underneath the surface. This

thickness is larger than the X-ray mean-penetration depth (around 1 μm) calculated for our experimental conditions.

For the 2.89 at. % Mg alloy, when the theoretical oxidation front is located at about 1.2 μm underneath the surface, the oxidation-front velocity, derived by the simplified relation $V = C_o D_o / C_{Mg} \eta \zeta$, is estimated to be 0.6×10^{-7} cm/s^{-1}, and the extra peak of the expanded layer appears.

For the dilute alloy (0.29 at.% Mg), after 6 min, the peak of the expanded layer appears; the theoretical depth is then situated at about 2.3 μm underneath the surface. At this distance the calculated velocity is 3.2×10^{-7} cm/s^{-1}.

For the two alloys, we can conclude that the zone, near the surface, investigated by X-ray diffraction measurements, is near completely "oxidized" in the form of hypo-stoichiometric clusters, before the appearance of the extra diffraction peak.

Coalescence of Hypo-Stoichiometric Clusters

It is established that rapid oxidant diffusion favors the formation of new elementary species rather than growth of existing clusters.

If we compare the last results, we note that the coalescence of the earlier clusters needs higher velocities of the oxidation front (i.e. high oxygen flux) for lower-solute alloys.

In the case of the dilute alloy (0.29 at.% Mg), the coalescence process gives rise to a low lattice-parameter expansion (about 0.17 %).

Kinetics studies give similar $C_0 D_0$ values in the two alloys during the first part of the coalescence process; the difference between the 0.29 Mg (1.59×10^{-15} cm^2/s) and the 2.89 Mg (7.24×10^{-15} cm^2/s) alloy could be dependent on different η values between the two alloys. These $C_0 D_0$ parameters are lower than the theoretical one established in pure silver [14] (4.73×10^{-13} cm^2/s). The noteworthy difference is explained by the later appearance of the expanded layer situated behind the oxidation front, during the first minutes. A high-oxygen flux allows the formation of hyper-stoichiometric clusters; the instability of these clusters depends on the amount of oxygen excess and on the number of Mg–O bonds. It was established that there is a limiting number of Mg–O bonds and that oxygen atoms are located at the periphery of the clusters.'

Hyper-Stoichiometric Cluster Evolution

This unstable configuration evolves toward close packing by contraction of the expanded layer and the release of an excess amount of oxygen.

The $C_0 D_0$ value calculated in the second part of the coalescence process for Ag-2.89 at.% Mg is very high (1.83×10^{-12} cm^2/s); this value is calcu-

lated assuming that the theoretical thickness varies as $\mathbf{t^{1/2}}$. The deviation to the Wagnerian behavior is in agreement with previous results [9] owing to faster kinetics and leading to the conclusion that the thickness of the expanded layer varies as $\mathbf{t^n}$ with $\mathbf{n} > 1$.

Lattice Parameter of the Unoxidized Matrix and Oxygen Excess

Solid-Solution Lattice Parameter

From the Mg concentrations reported in this study, the values of the lattice parameter of the unoxidized solid solution $a_{\mathrm{Ag(Mg)}}(T_0)$ at room temperature, T_0, according to Vegard's law, are 0.40872 nm (0.29 at.%) and 0.40987 nm (2.89 at.%). Using the following relation:

$$a_{\mathrm{Ag(Mg)}}(T) = a_{\mathrm{Ag(Mg)}}(T_0)\left[1 + \alpha_{\mathrm{Ag(Mg)}}(T - T_0)\right] \tag{7}$$

where $\alpha_{\mathrm{Ag(Mg)}} = 18.9 \times 10^{-6}\ \mathrm{K}^{-1}$ is the thermal-expansion coefficient of pure silver (assumed close to the alloy value), these values $a_{\mathrm{Ag(Mg)}}(T)$ reported at $T = 300°\mathrm{C}$ are, respectively, 0.41104 nm and 0.41219 nm.

The experimental values 0.41005 nm (0.29 at.%) and 0.41060 nm (2.89 at.%) obtained on the samples before the *in-situ* oxidation study, at 300°C are lower than the calculated lattice parameters. We can thus conclude that lattice parameters donot agree with the linear function of composition represented by Vegard's law. This assumption is in agreement with a previous study of Rikel and Goldacker[20] where the evolution of the silver lattice parameter with Mg content is described by the following expansion coefficient:$\alpha_{\mathbf{Mg}} = \delta\mathbf{a}/\delta\mathbf{C_{Mg}} = 0.011$ nm. Using this expression we now find lattice parameters of 0.41096 nm (0.29 at.% Mg) and 0.41126 nm (2.89 at.% Mg) at 300°C. These values are in much better agreement with experimental values ($\mathbf{\Delta a/a_{Ag}} = 0.16\%$ for the concentrated alloy and 0.22% for the dilute alloy) than those calculated from Vegard's law.

Oxygen Excess

The evolution from hypo- to hyper-stoechiometric clusters needs a significant trapping of oxygen atom s.[11,20,21] The oxidized-silver-layer expansion depends on the oxygen atom-to-magnesium atom ratio. The oxygen excess may be evaluated from the relation given by Rikel and Goldacker [20]:

$$a_{\mathrm{AgMgO}} = a_{\mathrm{Ag}} + \alpha_{\mathrm{MgO}} C_{\mathrm{MgO}} + \alpha_{\mathrm{O}} C_0^{\mathrm{excess}} \tag{8}$$

where the estimated values of the expansion coefficients are $\alpha_{\mathrm{MgO}} = 0.025 \pm 0.007$ nm and $\alpha_0 = 0.044 \pm 0.015$ nm for stoichiometric MgO and for the oxygen excess, respectively.

In the case of Ag-2.89 at.% Mg, the O/Mg ratio evolves between 4.45 at the very beginning of the experiment and 3.9 after 180 min. A similar value is reported by Rikel and Goldacker [20] from the data of our previous ex-situ studies,[9] obtained on Ag-1 at.% Mg polycrystalline samples (O/Mg $\approx$ 4.1). In a previous gravimetric study, on Ag-0.4 at.% Mg oxidized at 300°C under 1 atm. oxygen,[21] lower values were calculated during the coalescence process (O/Mg = 3.25).

For Ag-0.29 at.% Mg, a very large ratio (O/Mg $\approx$ 6.5) is calculated from the relation given by Rikel and Goldacker; the interstitial position of oxygen atoms in octahedral sites leads to a maximal value O/Mg = 6. Taking into account the low oxygen solubility in silver, a O/Mg ratio value larger than 6 is not realistic. In this dilute alloy, after 60 min, a small lattice relaxation occurs leading to a still large value (5.3) for the O/Mg ratio.

We believe that measured lattice parameters must be corrected from an elastic-strain effect. The out-of-plane, lattice-parameter mismatch between the undistorted zone and the distorted zone is about 0.2% for the dilute Ag alloy. It is lower than the value deduced from the yield stress (0.35%). It means that the elastic strain part in the measured out-of-plane lattice parameter can not be neglected. If we assume that the stress into the undistorted zone is due to the volume change between the "oxidized" silver and the initial Ag–Mg alloy, the maximum in-plane strain is then given by the Pilling–Bedworth ratio, i.e. :

$$\varepsilon_{//} = \frac{1}{3}\frac{\Delta V}{V} = \frac{\Delta a}{a} = \frac{a^{\mathrm{u}} - a^{\mathrm{d}}}{a^{\mathrm{a}}} \tag{9}$$

where a^{u} and a^{d} are the lattice parameters of the undistorted and distorted zone, respectively.

It gives − 0.22% and − 1.25% for the dilute alloy and for the more-concentrated one, respectively.

The out-of-plane strain is related to the in-plane strain through the following equation (assuming a biaxial state of stress)

$$\varepsilon_{\perp} = -\frac{2\nu}{1-\nu}\varepsilon_{//} \tag{10}$$

In terms of lattice parameter, it leads to:

$$a_0 = a_{\perp} - \frac{2\nu}{1+\nu}(a_{\perp} - a_{//}) \tag{11}$$

where $a_{//} = a^{\mathrm{u}}, a_{\perp}$ is the measured out-of-plane lattice parameter and a_0 the stress-free lattice parameter of the distorted zone.

For the dilute alloy, the in-plane strain induced by the volume change (– 0.22%) is lower than the yield strain of the material (0.35%). We can then assume that the distorted layer is fully strained by the volume change. As a consequence, we calculated for this alloy, using Eq.11, a stress-free lattice parameter of 0.41037 and 0.41033 nm at the beginning and at the end of the experiment, respectively. On the contrary, for the 2.89 Mg alloy, the maximum in-plane strain is given by the yield strain, because it is lower than the value deduced from the Pilling–Bedworth ratio. The out-of-plane lattice parameter is then described by the following relation:

$$a_{\perp} = a_0 - \frac{2v}{1-v} a_0 \varepsilon_{//} \tag{12}$$

It gives for a_0 values of 0.41330 and 0.41275 nm at the beginning and at the end of the experiment, respectively.

With these corrected stress-free lattice parameters, we now find for the O/Mg ratio a maximal and a final value that are quite reasonable for the two samples. In the case of Ag-0.29 at.% Mg, they are $(O/Mg)_{max} = 3.8 \pm 1$ and $(O/Mg)_{min} = 3.5 \pm 1$. For the Ag-2.89 Mg alloy, they are respectively $(O/Mg)_{max} = 3.4 \pm 0{,}8$ and $(O/Mg)_{min} = 2.9 \pm 0{,}8$. The standard deviations calculated here are deduced from the uncertainties on α_0.[20]

Within the accuracy indicated for the α_0 value cited above, we cannot conclude anything about the difference in the (O/Mg) values between the two alloys. Another reason to consider these results within some accuracy is that the expansion coefficient α_{MgO} is supposed to be of the same order as the expansion coefficient for Mg in Ag, α_{Mg}.[20] With this assumption, the lattice distortion depends only on the oxygen excess, and stoichiometric MgO should not induce any distortion. We must also note that the large difference in Mg concentration between the two alloys studied here implies, for comparable (O/Mg) values, an oxygen quantity stored ten times lower in the Ag-0.29 Mg than in the Ag-2.89 Mg.

One should also note that all these results are in agreement with the published gravimetric data obtained by Semega *et al.* [21] on polycrystalline samples of Ag-0.4 at.% Mg oxidized under 1 atm.O_2, at 300°C. In this study, during the coalescence process, they found a maximal value of 3.25.

Finally, during the first stage of the coalescence process we find ($\boldsymbol{n}$ = O/Mg) > 1, which implies that the C_0D_0 values are much smaller than theoretical ones. From the calculated values it is then not possible to explain the difference between the two alloys. On the contrary, during the second stage of this process, the measured kinetics are faster than expected from Wagner's law (using a η value of 1), all the more for η value higher than 1. This fact can not be explained presently.

CONCLUSIONS

In-situ X-ray diffraction experiments were performed during the oxidation of Ag–Mg single-crystal alloys for two magnesium contents. The evolution of the (022) reflection of the Ag solid solution was monitored. A lattice distortion induced by the oxygen atoms embedded into the matrix was observed. Such a lattice distortion depends on an oxygen excess in hyper-stoichiometric MgO clusters. During the first stage of internal oxidation, the oxygen diffusivity in silver, C_0D_0, is slightly lower than the theoretical one. In the second stage, accelerated kinetics give rise to a very high C_0D_0 value at variance with a Wagnerian behavior.

O/Mg atomic ratios are deduced from the lattice-parameter changes. Taking into account the elastic strain between the oxidized zone and the unoxidized zone, the O/Mg ratios are in agreement with the values obtained in previous studies.

REFERENCES

1. J.L. Meijering, and M.J. Druyvesteyn, *Philips Research Report* **2**, 81 (1947).
2. M. Sato, *Transactions of the Japanese Institute of Metallurgical* **23**, 480 (1982).
3. J.L. Brimhall, and R.A. Huggins, *Transaction of the Metallurgical Society of AIME* **233**, 1076 (1965).
4. C. Wagner, *Elektrochemical* **63**, 772 (1959).
5. J.S. Hirschhorn, and F.V. Lenel, *Transactions of the ASM* **59**, 208 (1966).
6. H.H. Podgurski, and F.N. Davis, *Transactions of the Metallurgical Society of AIME* **230**, 731 (1964).
7. R. Lacroix, *Memories Scientifique's Revue Metallurgic* **63**, 693 (1966).
8. J.S. Hirschhorn, *Journal of Metallurgical Science* **1**, 91 (1967).
9. L. Charrin, A. Combe, F. Cabane, and J. Cabane, *Oxidation of Metals* **40**(5–6), 483 (1993).
10. L. Charrin, A. Combe, J. Cabane, and A. Charaï, *La revue de métallurgie-CIT/Science des Matériaux* **May**, 669 (1998).
11. L. Charrin, A. Combe, and J. Cabane, *Oxidation of Metals* **8**, 65 (1992).
12. L. Charrin, A. Becquart-Gallissian, A. Combe, G. Gonzalez, and A. Charaï, *Oxidation of Metals* **57**(1/2), 81 (2002).
13. L. Charrin, A. Becquart-Gallissian, A. Combe, and A. Charaï, *Scripta Materials* **42**, 701 (2000).
14. W. Eichenauer, and G. Müller, *Zeitschrift Fur Metallkunde* **53**, 321 (1962).
15. D.L. Douglass, *Oxidation of Metals* **44**(1/2), 81 (1995).
16. D.L. Douglass, *Journal of Oxidation of Metals* **November**, 74 (1991).
17. L. Charrin, A. Combe, A. Charaï, F. Cabane, and J. Cabane, *Journal of Physics IV* **4**, 41 (1994).
18. I. Noyan, and J. Cohen, *Residual Stress* (Berlin: Springer Verlag- Stuttgart, 1987).
19. K.C. Goretta, J.L. Routbort, R.L. Thayer, J.P. Carroll, J. Wolfenstine, J. Kessler, and J. Schwartz, *Physica C* **265**, 201 (1996).
20. M.O. Rikel, and W. Goldacker, *Journal of Materials Research* **14**, 2436 (1999).
21. M.B. Semega, L. Charrin, and A. Combe, *Journal of Philosophical Magazine A* **66**, 1139 (1992).